Pervaporation Separation of IPA-Water Mixtures Through 4A Zeolite-Filled Sodium Alginate Membranes

H. Sudhakar,[1] C. Venkata Prasad,[1] K. Sunitha,[2] K. Chowdoji Rao,[1] M. C. S. Subha,[3] S. Sridhar[2]

[1]*Department of Polymer Science and Technology, Sri Krishnadevaraya University, Anantapur 515 003, India*
[2]*Membrane Separations Group, Chemical Engineering Division, Indian Institute of Chemical Technology, Hyderabad 500 007, India*
[3]*Department of Chemistry, Sri Krishnadevaraya University, Anantapur 515 003, India*

Received 14 July 2010; accepted 5 November 2010
DOI 10.1002/app.33695
Published online 29 March 2011 in Wiley Online Library (wileyonlinelibrary.com).

ABSTRACT: Incorporation of zeolites into natural polymers has been shown experimentally to enhance both the flux and selectivity in pervaporative dehydration separation of organic compounds. Pervaporation is a promising membrane technique for separation of volatile organic compounds (VOCs)/water mixtures. In this study, hydrophilic sodium alginate (SA) mixed membranes were prepared using solution casting technique by incorporating zeolites into the polymer matrix. The prepared membranes were characterized by ATR-Fourier transform infrared spectroscopy (FTIR), X-ray diffraction (XRD), scanning electron microscopy (SEM), Thermal Gravimetric Analysis (TGA), and differential scanning calorimetry (DSC) were tested in a laboratory scale pervaporation experimental set-up. The effect of experimental parameters such as the type and composition of zeolites on permeation flux and selectivity was investigated. When tested on IPA-water mixtures, the zeolite-filled membrane was found to give much higher selectivity.
© 2011 Wiley Periodicals, Inc. J Appl Polym Sci 121: 2717–2725, 2011

Key words: pervaporation; sodium alginate; glutaraldehyde; 4A zeolite; isopropanol-water

INTRODUCTION

Pervaporation (PV) technique has a great deal of potential application in separation technology where the conventional techniques (reverse osmosis and distillation) are not possible. This includes the separation of azeotropes: mixture of components with a slight difference in volatility, and the components that are pressure or temperature sensitive. These separations occur in (petro) chemical as well as food industry and in waste water treatment.[1–4] For dehydration purposes, hydrophilic membranes are used. Up to now, mostly polymeric membranes have been used on an industrial scale.

Zeolites have unique properties that are very attractive features due to their well-defined micropore structure, good thermal and structural stability, high mechanical strength, feasible to steady-state operation, low energy consumption, resistance to relatively extreme chemical environment.[5–9] In particular, the acid sites due to the presence of aluminum, the high specific surface, and the well-defined pore dimensions have imposed them as selective catalytic materials. Zeolite-filled membranes have been widely used in boosting the PV separation characteristics over neat polymer membranes.

Earlier reports have been devoted to molecular-based separations using zeolite-filled polymeric membranes in liquid separations. Zeolites are crystalline, microporous aluminosilicates which find extensive industrial usage as catalysts, adsorbents, and ion exchangers with high capacities and selectivities.[10,11] The characteristics of zeolite membrane have found its new application in gas, vapor, and liquid separation especially in petrochemical industry based on their properties, Viz., adsorption, preferential diffusion or molecular sieving.[12–15] Besides, membranes composed of different types of zeolite provide different framework structure and pore size, which make it suitable as a membrane reactors, catalytic membrane reactor, sensitive chemical sensors, reactive and nonreactive gas sensors, electronic and thermo electronic applications such as zeolite-based capacitors [7,9,12,16]

Currently, zeolite membranes have been found in the literature because of its promising applications in corrosion protection and antimicrobial coatings.[17,18] The crystalline nature of zeolites offers the opportunity to obtain membranes with a regular 3D network of micropores at a molecular scale and are therefore able to separate mixture of substances on the basis of differences in the molecular size and shape,[19] such

Correspondence to: K. Chowdoji Rao (chowdojirao@gmail.com).
Contract grant sponsor: UGC New Delhi (UGC-RGNF); contract grant number: F.16-89/2006(SA-II).

© 2011 Wiley Periodicals, Inc.

as, for example, isomers[12] (compounds with similar molecular weight) and azeotropic mixtures.[20] The advantage of using a zeolite membrane is that it can potentially separate molecules in a continuous way. For example, modules of hydrophilic zeolite A (LTA) membranes were recently commercialized for alcohol dehydration by pervaporation.[21] Incorporation of zeolite or porous fillers in dense membrane can improve the separation performance[22,23] due to combined effect of molecular sieving action, selective adsorption, and difference in diffusion rates. Sodium alginate has excellent good chemical resistance and mechanical strength. However, the low permeation rate should be overcome while it is used as a membrane material for pervaporation separation. Thus, in this study, hydrophilic zeolite 4A (particle size: 4.33 μm, pore size: 3.8 Å, Si/Al ratio: 1) were introduced in the sodium alginate (SA) matrix. It was expected to improve the permeation rate due to molecular sieving effect and hydrophilicity of the zeolites.

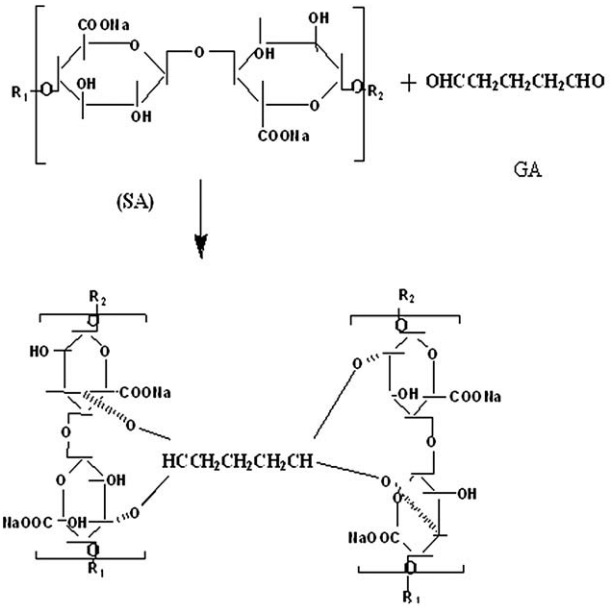

Figure 1 Reaction scheme of SA cross linked with glutarldehyde.

EXPERIMENTAL

Materials

Sodium alginate (SA), Isopropanol (IPA), hydrochloric acid (HCl), and glutaraldehyde (GA) were purchased from s.d. fine Chemicals, Mumbai, India. The 4A zeolite was kindly supplied by M/S Zeolite and Allied products, Mumbai. All the chemicals were of reagent grade and used without further purification. Deionized water generated by RO system was used throughout the research work.

Membrane preparation

SA (2 g) was dissolved in 100 mL of deionized water in conical flask at constant stirring for about 24 h at room temperature. The solution was then filtered to separate any undissolved matter and obtain bubble-free solution. The resulting homogeneous solution was spread onto a glass plate with the aid of a casting knife in a dust-free atmosphere at room temperature. After being dried for about 48 h, the membrane was subsequently peeled-off.

To prepare zeolite-incorporated SA membrane, a known amount of 4A (10, 20, and 30 wt %) zeolite was added into a sodium alginate solution. The amount of sodium alginate was kept constant for each membrane. The mixed solution was stirred for about 24 h and then kept in an ultrasonic bath for about 30 min to break the aggregated zeolite particles so as to improve the dispersion of zeolite in the polymer matrix. The resulting solution was poured onto a glass plate and the membrane was dried to constant weight. The prepared membranes were then crosslinked in a crosslinking bath containing 84 vol % isopropanol, 10 vol % water, 5 vol % of glutaraldehyde as a crosslinker, and 1 vol % hydrochloric acid as a catalyst for a period of 2 h. The amount of 4A zeolite with respect to SA varied from 0 to 30 wt % and the membranes thus obtained were designated as *SA*-0, *SA*-10, *SA*-20, and *SA*-30, respectively. The schematic representation of crosslinking reaction of SA with GA is shown in Figure 1.

Membrane characterization

Membranes used in the present study were characterized using the following techniques.

Fourier transform-infrared (FTIR) spectroscopic studies

Pure SA, crosslinked SA, and 4A zeolite incorporated SA membranes were scanned equipped using FTIR spectrometer (Bomem MB: 3000, Canada), equipped with attenuated total reflectance (ATR). Dry membranes were characterized in the range of 4,000–500 cm^{-1} at a scan rate of 25 cm^{-1} under N_2 atmosphere.

X-ray diffraction (XRD) analysis

A Siemens D 5000 (Germany) X-ray diffractometer was used to study the crystallinity of SA and zeolite filled SA membranes. X-rays of 1.5406 Å wavelength was generated by a Cu Kα source. The angle of diffraction was varied from 2° to 65° to identify changes in the crystal structure and intermolecular distances between intersegmental chains after modification.

SEM Studies

Scanning electron micrographs (SEM) of surface and cross section were taken for the zeolite-filled SA membranes; using software controlled digital scanning electron microscope-JEOL JSM 5410, Japan.

Thermogravimetric analysis (TGA) studies

Thermal stability of the polymer membranes was studied using TG instruments (Model: SDT Q600, U.K) in the temperature range of 25–600°C at a heating rate of 10°C min^{-1}, under N_2 atmosphere (100 mL min^{-1}). Samples were subjected to TGA before and after incorporation of zeolite to determine the thermal stability and decomposition characteristics.

Differential scanning calorimetry (DSC) studies

DSC curves of the polymer membranes was examined using TG instruments (Model: SDT Q600, U.K) in the temperature range of 25–600°C at a heating rate of 10°C min^{-1}, under N_2 atmosphere (100 mL min^{-1}). The samples were subjected to DSC before and after incorporation of zeolite to determine the thermal stability and decomposition characteristics.

Mechanical properties studies

Mechanical strength of the membranes was performed at room temperature using Universal testing machine (Instron-UK) with an operating head load of 5 kN at the rate of 12.5 mm min^{-1}. Cross-sectional area of the sample of known width and thickness was calculated. Tensile strength was calculated using the following.

$$\text{Tensile strengh} = \frac{\text{Max load}}{\text{cross sectional area}} \text{N/mm}^2 \quad (1)$$

Pervaporation experiments

The equipment (Fig. 2) used to perform the PV experiments remained the same as described in the earlier studies.[24] The pervaporation cell consist of two bell-shaped B-24 size glass column reducers/couplers clamped together with external padded flanges by means of tie rods to give a vacuum tight arrangement. The top half was used as a feed chamber and the bottom one as a permeate chamber. The membrane was supported by a stainless steel porous plate which was embedded with a mesh of the same material to provide a smooth uniform surface. Teflon gaskets were fixed by means of high vacuum silicone grease on either side of the membrane and the sandwich was placed between the two glass column couplers and secured tightly. The effective membrane area that was in contact with the feed

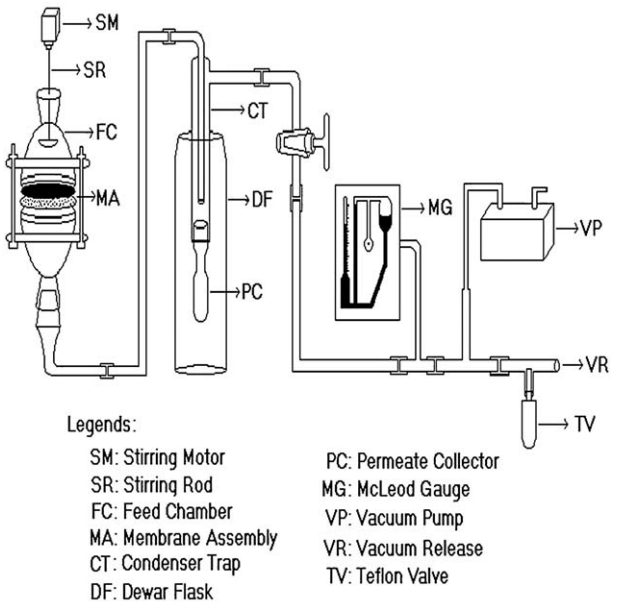

Figure 2 Schematic diagram of laboratory pervaporation set-up.

was 20 cm^2. After fixing the membrane, the cell was installed in the manifold and connected to the permeate line by means of a B-24 glass cone which was fixed to a high vacuum glass valve on one side followed by a glass condensor trap which consists of a small detachable collector. The trap was placed in a Dewar flask containing liquid nitrogen for condensing the permeate vapors. A rotary vacuum pump was used to maintain the permeate side pressure which was measured with an Edward's Mcleod gauge of scale in the range 0.01–10 mmHg. High vacuum rubber tubing was used to connect the various accessories to the experimental manifold. All glass cone-socket joints were fixed with good quality high vacuum grease (Dow Corning, USA).

Initially the membrane was soaked in the feed solution overnight to attain equilibrium. During the experiments the membrane upstream side was maintained at atmospheric pressure and the downstream side pressure was controlled by adjusting the value for vacuum release (vent). Permeate was condensed in the trap for a period of 6–8 h and then collected in a sample bottle for evaluation of its weight to determine the flux and analyzed by gas chromatography to calculate the selectivity. Flux (J_i) was calculated using eq. (2). The feed was kept in continuous stirring mode using an overhead stirring motor to minimize concentration polarization.

$$J_i = \frac{W_i}{At} \quad (2)$$

Here W_i represents the mass of water in permeate (kg), A is the membrane area (m^2) and t represents the permeation time (h).

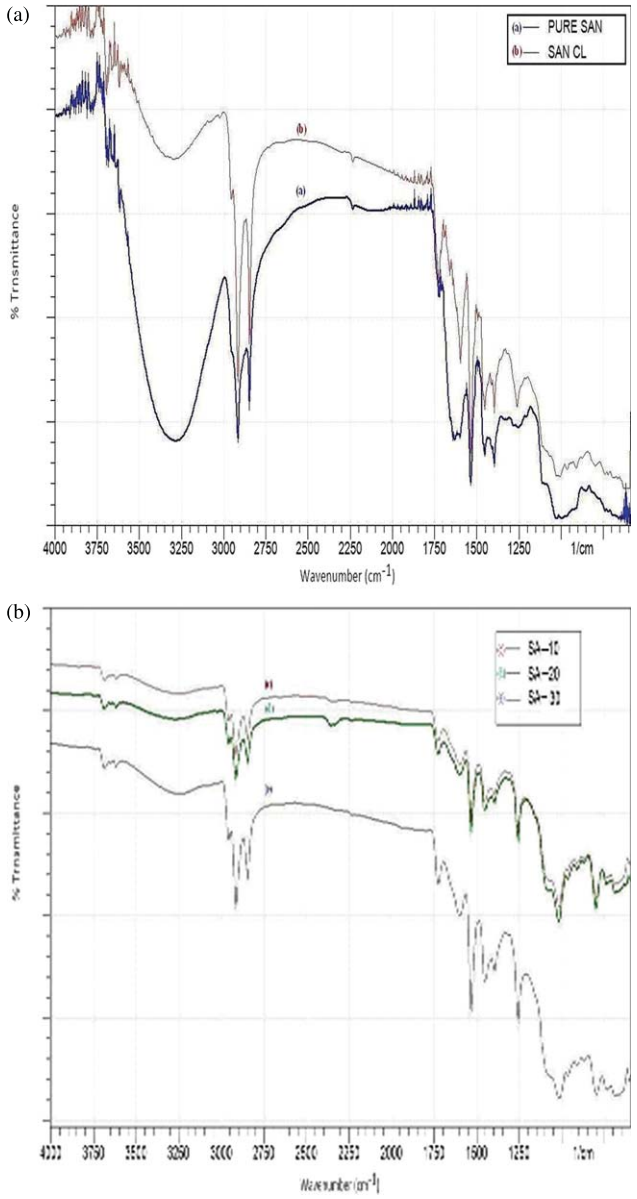

Figure 3 (A) FTIR spectra of (a) Pure SA and (b) cross linked SA membranes. (B) FTIR spectra of zeolite-filled crosslinked membranes (c) SA-10; (d) SA-20; and (e) SA-30. [Color figure can be viewed in the online issue, which is available at wileyonlinelibrary.com.]

The composition of both feed and permeate was determined using a Nucon gas chromatograph (Model 5765) installed with thermal conductivity detector (TCD) and packed column of 10% diethylene glycol sebacate (DEGS) on 80/100 Supelcoport of 1/8″ internal diameter and 2 m length. Temperature was maintained at 70°C (isothermal) while the injector and detector temperatures were maintained at 150°C each. The sample injection size was 1 μL and pure hydrogen was used as the carrier gas at a pressure of 1 kg cm^{-2}. The GC response was calibrated for this particular column and conditions with known compositions of IPA-water mixtures and the calibration factors were fed into the software to obtain correct analysis of unknown samples, and the errors in the pervaporation measurements were less than 1.0%. The selectivity of 4A zeolite-filled membranes was evaluated by using eq. (3): Membrane selectivity, α, is the ratio of permeability coefficient of water to that of isopropanol, calculated from their respective weight concentrations in feed and permeate as given below:

$$\alpha = \frac{y(1-x)}{x(1-y)} \tag{3}$$

where y is the permeate weight fraction of the faster permeating component (water) and x is its feed weight fraction.

Sorption experiments

Interaction of the membranes with the pure liquid components of the feed mixture was determined by gravimetric sorption experiments. Dried membranes of known weight were immersed in different compositions IPA/water mixture for about 48 h. When the sample attained constant weight, the membrane was carefully wiped off with filter papers to remove surface adhered liquid, and weighed quickly. Degree of swelling was calculated using:

$$\text{Degree of swelling} = \frac{M_s}{M_d} \tag{4}$$

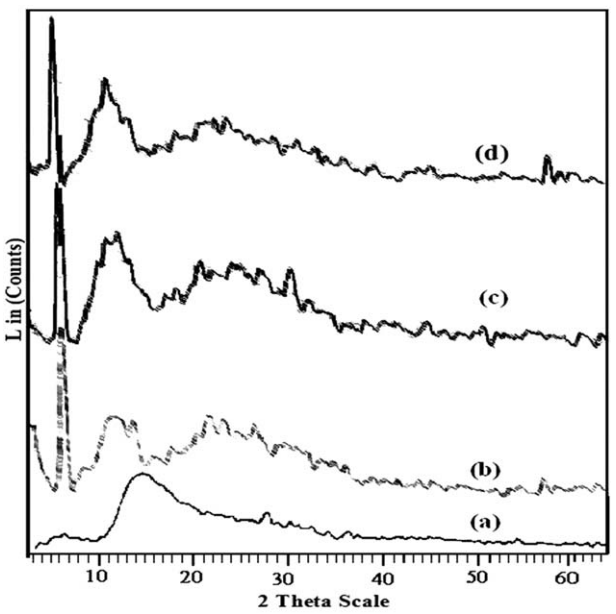

Figure 4 Wide angle X-ray diffraction patterns of zeolite-filled SA membranes: (a) SA-0; (b) SA-10; (c) SA-20; and (d) SA -30.

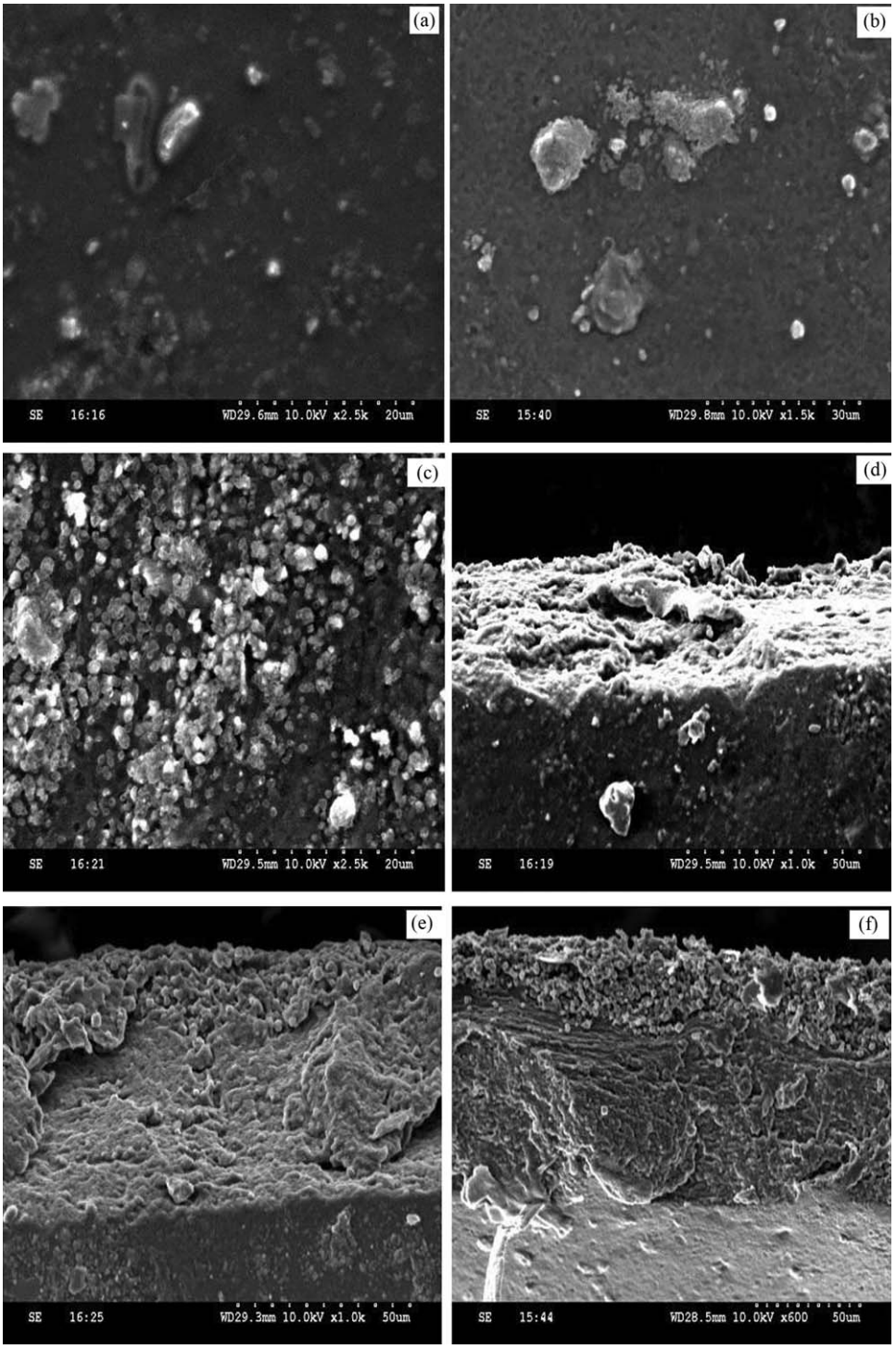

Figure 5 (A) SEM pictures Surfaces of the: (a) SA-10; (b) SA-20; and (c) SA-30. (B) SEM pictures of the (cross section): (d) SA-10; (e) SA-20; and (f) SA-30.

where M_s is mass of the swollen membrane in (g) and M_d is mass of the dry membrane in (g). The percent sorption was calculated using the equation:

$$\% \text{ Sorption} = \left[\frac{M_s - M_d}{M_d}\right] \times 100 \quad (5)$$

RESULTS AND DISCUSSION

Membrane characterization

FTIR analysis

The FTIR spectra of uncrosslinked [Fig. 3(A(a))] and crosslinked [Fig. 3(A(b))] membranes are shown in Figure 3(A). From Figure 3(A), two strong absorption

TABLE I
Thermal Stability Data of SA-4A Zeolite Membranes

Weight % of zeolite	Temperature for 50 wt % loss in °C
0	250
10	262
20	322
30	390

peaks at 1609 and 1416 cm^{-1} are seen. They can be assigned to the asymmetric and symmetric stretching vibration of the carboxylate group, respectively,.[25,26] It is revealed from this spectrum [Fig. 3(A)] a peak at 3320 cm^{-1} exhibits corresponding to O—H stretching vibrations of SA. Curve, at 1630 cm^{-1} has a broad band; this refers to carboxyl groups of —COONa of SA. The weak band at around 2930 cm^{-1} which corresponds to aliphatic C—H stretching and two strong bands at 1090 and 1034 cm^{-1} corresponds to C—O stretching are noticed.

In crosslinked curve [Fig. 3(A(b))] the peak observed at 3320 cm^{-1} confirms the of O—H groups of SA, during crosslinking reaction. A sharp peak at 1270 cm^{-1} further refers to C—O stretching vibration due to crosslinking reaction with glutarldehyde. In addition to this, Figure 3(B) shows a strong peak observed at around 1020 cm^{-1} is assigned to C—O stretching of SA. The Si—O band[27] also appeared at the same wavelength upon loading zeolite in the polymer matrix and hence, C—O and Si—O bands are almost overlapping in the spectra. From Figure 3(B) it is also observed that with increase of zeolite in the filled membrane percentage of transmission also decreases, this indicates the increase adherence between SA and zeolite.

X-ray diffraction

To monitor the effect of zeolite on degree of crystallinity of a polymer system it is of great significance in understanding the separation characteristics of the membranes in the PV process. The degree of crystallinity of SA [Fig. 4(a)] and 4A zeolite-filled SA membranes [Fig. 4(b)] was investigated by X-ray diffraction technique ($2\theta = 2–60°$). The results obtained for *SA*-10 to *SA*-30 series are shown in Figure 4. For the loosely packed *SA*-10, considerable amount of free volume may exist within the polymer matrix. Thus, the general shapes of the XRD pattern of zeolite-filled SA membranes are very similar, but the sharp peak is observed depending upon the zeolite content. In contrast, Figure 4(b) shows the crystallinity of zeolite-filled *SA*-10 membranes decreased significantly compared with that of the *SA*-30 membrane. This indicates with increase in zeolite content in the membrane matrix the crystallinity also increases i.e., evident from Figure 4.

SEM analysis

Figure 5(A) shows SEM surface images of typical 4A zeolite-filled SA membranes. All zeolite-filled membranes appear to be smooth and dense. The zeolite crystals are clearly visible. Figure 5(B) shows, side view images of 4A zeolite-filled SA membranes. The dispersion trend of zeolite particles in the polymer matrix are also observed from the SEM images. Zeolite showed excellent dispersion in the polymer matrix which is responsible for high selectivity of the membrane.

TGA studies

The thermo gravimetric analysis of SA and 4A zeolite-filled SA membranes are determined and discussed here. Thermal stability refers to the weight of zeolite and the temperature at which 50% weight loss given in Table I. Figure 6 illustrates the weight loss of sodium alginate zeolite composite membranes as a function of temperature. From the Figure 6 it is also noticed that thermogravimetric analysis of SA and 4A zeolite-filled SA composite membranes enhance an increase in the thermal stability of the polymer. The results of TGA are presented in Table I.

The increase in the thermal stability of SA-4A zeolite composite membranes with an increase in zeolite loading is due to the adsorption of polymer chains on the zeolite surface. These adsorbed polymer chains on a zeolite surface form a complex and the polymer chains which are away from the activated surfaces degrades faster. The adsorbed polymer chains hinder the diffusion of volatiles from the

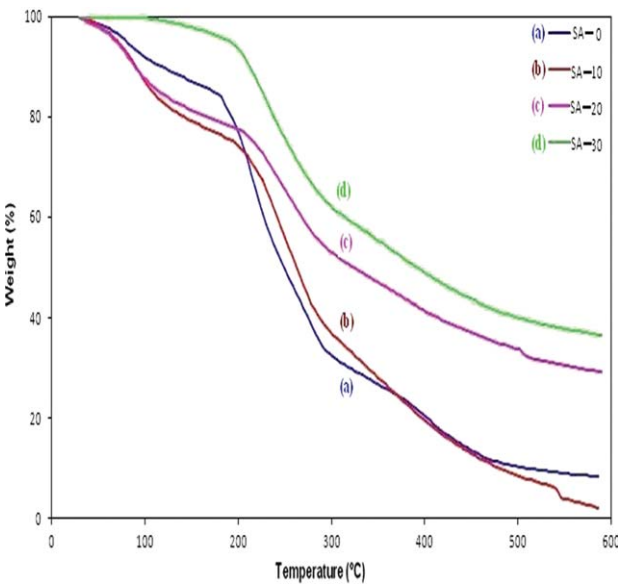

Figure 6 TGA analysis of (a) SA-0; (b) SA-10; (c) SA-20; and (d) SA-30. [Color figure can be viewed in the online issue, which is available at wileyonlinelibrary.com.]

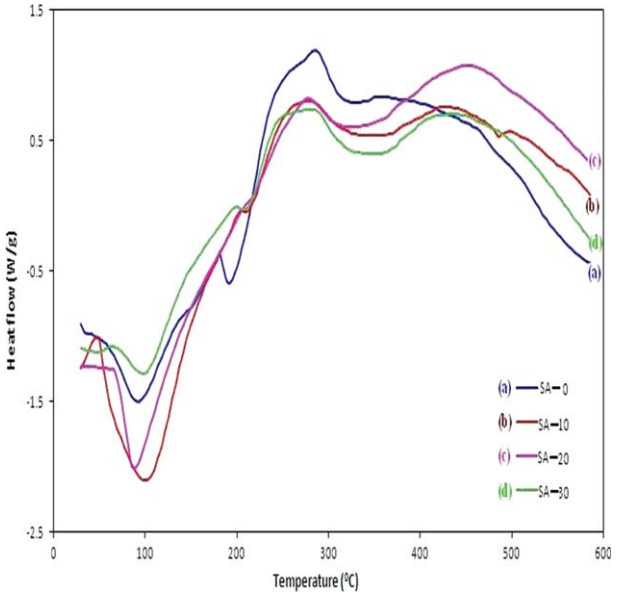

Figure 7 DSC curves of (a) SA-0; (b) SA-10; (c) SA-20; and (d) SA-30. [Color figure can be viewed in the online issue, which is available at wileyonlinelibrary.com.]

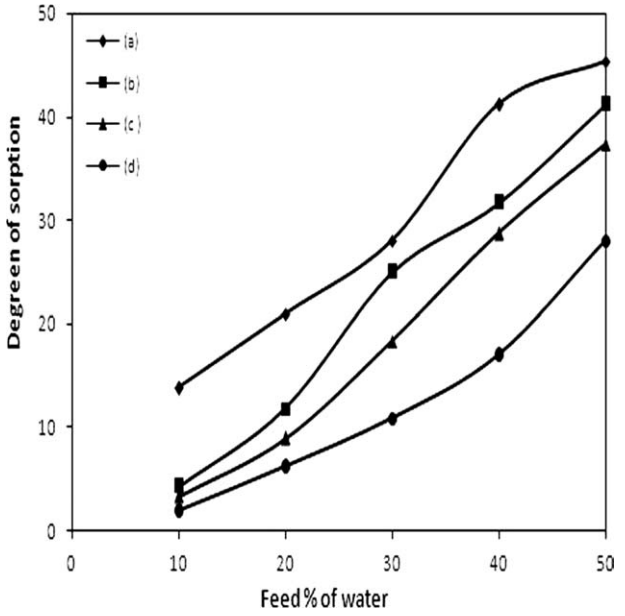

Figure 8 Plots of degree of sorption vs. percentage of water (a) SA-0; (b) SA-10; (c) SA-20; and (d) SA-30 incorporated 4A zeolite crosslinked membranes.

polymer resulting in the enhancement of thermal stability of sodium alginate membrane.

DSC studies

DSC curves of pure SA and zeolite-filled SA membranes are shown in Figure 7. DSC curve of SA membrane shows an endothermic peak at 190°C, corresponding to its melting point. The melting endotherm has shifted to higher temperatures, viz., 210–230°C, for 10–30 wt % zeolite loaded SA membranes. It is evident from Figure 7 that the zeolite-filled membranes have higher melting temperatures, melting temperature (T_m) of SA mixed matrix membranes also increases.

Mechanical properties

SA-0, *SA*-10, *SA*-20, and *SA*-30 crosslinked membranes exhibited tensile strengths of 16.42, 20.13, 21.95, and 25.68 N mm^{-2} respectively, calculated from the stress–strain curves, which showed an enhancement in mechanical strength on incorporation of zeolite (Table II). The XRD spectra confirmed the increase in crystallinity of SA after incorporating

TABLE II
Tensile Strength of SA and 4A Zeolite Incorporated Polymer Membranes

Membrane	Tensile strength (N mm^{-2})
SA-0	16.42
SA-10	20.13
SA-20	21.95
SA-30	25.68

TABLE III
Effect of Feed Composition on Separation Performance of SA and Zeolite-Filled SA Membranes (Permeate Pressure 1 mmHg) at 30°C

Feed compositions		Permeate compositions (wt %)			
Water (x)	IPA ($1-x$)	Water (y)	IPA ($1-y$)	Selectivity α	Flux (kg m^{-2} h^{-1})
SA-0					
4.561	95.439	98.214	1.786	798.53	0.18
9.865	90.135	96.785	3.215	455.82	0.20
20.123	79.877	94.687	5.313	359.54	1.78
29.145	70.855	93.749	6.251	253.89	3.65
40.012	59.988	89.357	10.643	152.36	7.38
51.236	48.764	86.679	13.321	102.89	11.68
SA-10					
5.236	94.764	99.128	0.872	874.36	0.13
10.012	89.988	98.044	1.956	655.82	0.45
19.689	80.311	97.982	2.018	519.25	3.65
28.145	71.855	96.851	3.149	421.25	5.68
39.896	60.104	92.377	7.623	389.36	8.24
48.965	51.035	90.767	9.233	355.82	14.58
SA-20					
4.869	95.131	99.894	0.106	1358.93	0.25
11.235	88.765	99.251	0.749	986.32	1.97
20.178	79.822	98.356	1.644	889.25	5.68
29.635	70.365	96.352	3.648	824.24	11.23
39.854	60.146	94.014	5.986	712.32	13.25
49.632	50.368	93.358	6.642	658.75	18.65
SA-30					
5.369	94.631	99.868	0.132	1857.36	0.04
10.124	89.876	99.601	0.399	1458.23	2.21
19.457	80.543	98.657	1.343	1524.32	8.65
29.927	70.073	98.014	1.986	1098.36	14.35
38.954	61.046	97.587	2.413	905.24	19.85
49.479	50.521	96.869	3.131	874.25	24.35

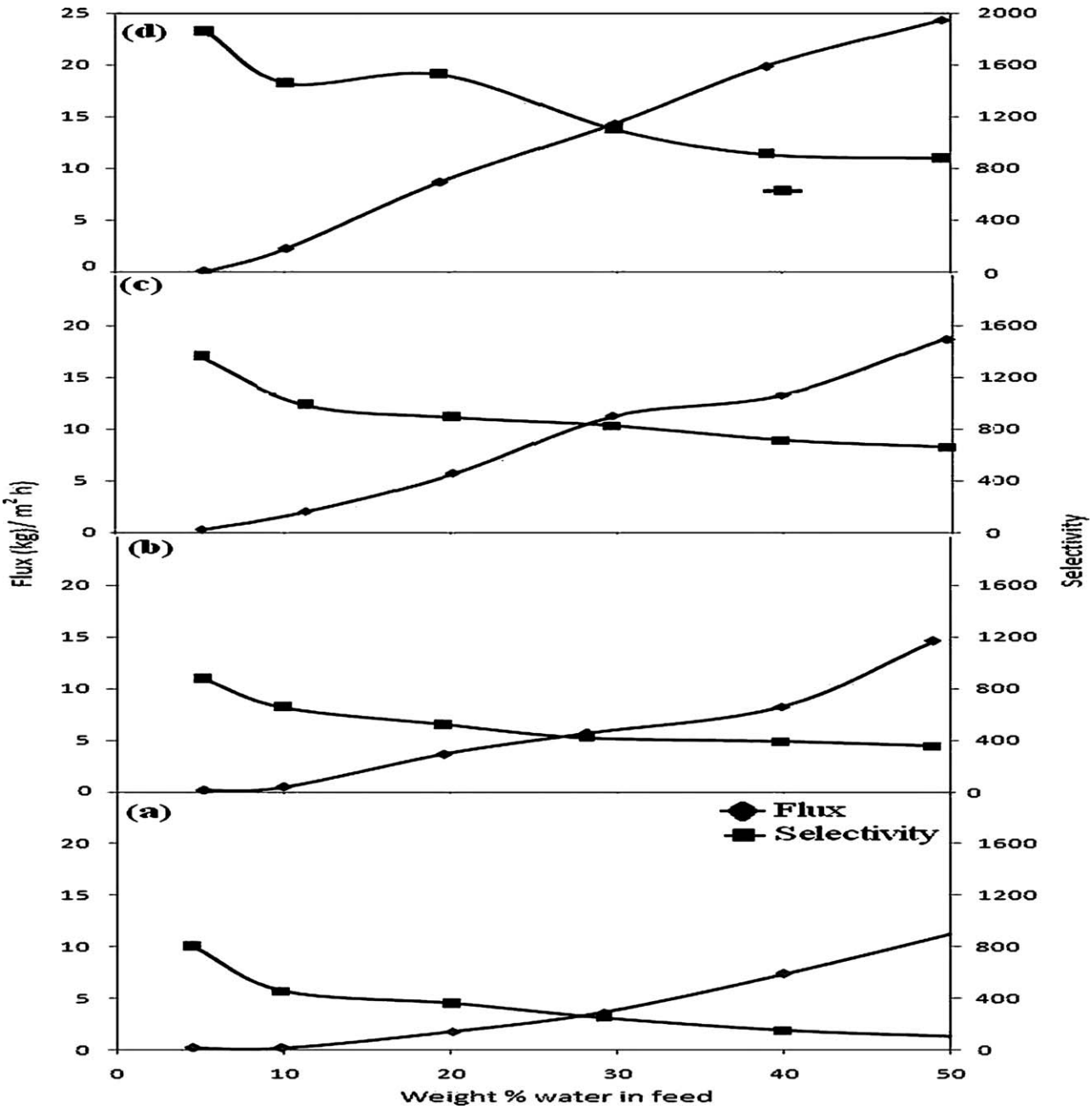

Figure 9 Effect of feed compositions on pervaporation performance of (a) SA-0; (b) SA-10; (c) SA-20; and (d) SA-30 incorporated zeolite crosslinked membranes.

zeolite. Extensive intra- and intermolecular hydrogen bonds in sodium alginate, besides the formation of an interpenetrating polymer network upon crosslinking is also responsible for such increase in mechanical strength. Thus, mechanical strength of the membranes increased on increasing the zeolite content in the membrane.

Sorption studies

From sorption studies, the amount of water sorbed by the membranes was investigated at different compositions of IPA/water mixtures. The results indicate that swelling behavior of a preferential component affects the membrane performance. This property depends on the nature of membrane material and the membrane preparation conditions. The swelling property for the unmodified and the modified SA membranes are shown in Figure 8.

From Figure 8, it is clearly seen that pure SA and zeolite-filled SA membranes, the degree of swelling increases with increasing water concentration in water/IPA mixture. By comparison, the modified membranes have a lower degree of swelling than that of unmodified membranes. Modification of SA mixed matrix membranes via chemical crosslinking resulted in a more compact structure and therefore

the membrane acquire less affinity and less sorption ability.

Pervaporation properties

The data pertaining to pervaporation results of IPA-water mixtures through 4A zeolite-filled SA membranes are given in Table III. It has been widely accepted that under reduced pressure conditions the transport of a volatile organic mixtures through a PV membrane comprises of three steps: a sorption step at the membrane upstream face, followed by diffusion through the polymer film and desorption into the vacuum. Under high vacuum, on the downstream side of the polymer film, the desorption is considered a fast step. Therefore, the overall separation characteristic of a membrane depends on delicate balance of three intrinsic properties of the penetrants of the mixture: affinity to the membrane, the size of the penetrating molecules and their vapor pressure. Considering the pervaporation separation of aqueous IPA solutions, the relative affinity of IPA and water molecules to the membrane could be assessed experimentally by sorption measurements. To match our anticipation, by incorporation of zeolite with SA, the selectivity of all zeolite-filled SA membranes was found to be enhanced proportional to the amount of the zeolite added (Table III). The PV results are corelated with results obtained in sorption studies. From this result it is also observed that the small pore size of 4 Å might also favor the preferential permeation of water molecules. The complementary effects of the zeolite on sorption and diffusion would improve membrane performance in terms of both flux and selectivity.

Membrane performance was studied using flux and selectivity data generated at 30°C and displayed in Figure 9. The flux increased and the selectivity decreased with increasing feed water content, which is attributed to the hydrophilicity of the membranes. The increasing water content makes the membranes become more swollen; hence, this is responsible for increase in flux and decrease in selectivity. From Figure 9, it can also be noticed that when zeolite content is 30 wt %, the flux of *SA*-30 membrane is higher than that of *SA*-0 membrane, and the selectivity of *SA*-30 membrane is slightly increased when compared to *SA*-0 membrane.

CONCLUSION

From PV results it is concluded that the modification of SA membranes with suitable amount of hydrophilic zeolite (4A) is an effective means to improve IPA/water separation (i.e., selectivity and flux). As compared with the zeolite free membrane, 4A zeolite filled membranes of the study are mechanically strong and are able to withstand for PV conditions. With increase in water content of the feed, flux increases whereas the selectivity decrease which can be attributed to the hydrophilicity nature of zeolite.

References

1. Garcia Villaluenga, J. P.; Tabe-Mohammadi, A. J Membr Sci 2000, 169, 159.
2. Lipnizki, F.; Field, R. W.; Ten, P. K. J Membr Sci 1999, 153, 183.
3. Sampranpiboon, P.; Jiraratananon, R.; Uttapa, D.; Feng, X.; Huang, R. Y. M. J Membr Sci 2000, 174, 55.
4. Kujawski, W. Polish J Env Stud 2000, 9, 13.
5. Motuzas, J.; Julbe, A.; Noble, R. D.; Guizard, C.; Beresnevicius, Z. J.; Cot, D. Micropor Mesopor Mater 2005, 80, 73.
6. Shan, W.; Zhang, Y.; Yang, W.; Ke, C.; Gao, Z.; Ye, Y.; Tang, Y. Micropor Mesopor Mater 2004, 69, 35.
7. Bernal, M. P.; Xomeritakis, G.; Tsapatsis, M. Catal Today 2001, 67, 101.
8. Bonilla, G.; Vlachos, D.; Tsapatsis, M. Micropor Mesopor Mater 2001, 42, 191.
9. Deshayes, A. L.; Miro, E. E.; Horowitz, G. I. Chem Eng J 2006, 122, 149.
10. Bhat, S. D.; Aminabhavi, T. M. J Appl Polym Sci 2009, 113, 157.
11. Wee, S. L.; Tye, C. T.; Bhatia, S. Sep Purif Technol 2008, 63, 500.
12. Nair, S.; Lai, Z.; Nikolakis, V.; Xomeristakis, G.; Bonilla, G.; Tsapatsis, M. Micropor Mesopor Mater 2001, 48, 219.
13. Lai, Z.; Tsapatsis, M. Ind Eng Chem Res 2004, 43, 3000.
14. Keizer, K.; Burggraaf, A. J.; Vroon, Z. A. E. P.; Verweij, H. J Membr Sci 1998, 147, 159.
15. Gump, C. J.; Tuan, V. A.; Noble, R. D.; Falconer, J. L. Ind Eng Chem Res 2001, 40, 565.
16. De La Iglesia, O.; Hirsuta, S.; Mallada, R.; Menendez, M.; Coronas, J.; Santamaría, J. Micropor Mesopor Mater 2006, 93, 318.
17. Cheng, X.; Wang, Z.; Yan, Y. Electrochem Solid State Lett 2001, 4, B23.
18. McDonnell, A. M. P.; Beving, D.; Wang, A.; Chen, W.; Yan, Y. Adv Funct Mater 2005, 15, 336.
19. Caro, J.; Noack, M.; Kolsch, P.; Schafer, R. Micropor Mesopor Mater 2000, 38, 3.
20. Coronas, J.; Santamaría, J. Sep Purif Methods 1999, 28, 127.
21. Morigami, Y.; Kondo, M.; Abe, J.; Kita, H.; Okamoto, K. Sep Purif Technol 2001, 25, 251.
22. He, X.; Chan, W. H.; Ng, C. F. J Appl Polym Sci 2001, 82, 1323.
23. Kittur, A. A.; Kariduraganavar, M. Y.; Toti, U. S.; Ramesh, K.; Aminabhavi, T. M. J Appl Polym Sci 2003, 90, 2441.
24. Sudhakar, H.; Chowdoji Rao, K.; Sridhar, S. Des Monom Polym 2010, 13, 287.
25. Rao, C. N. R. Chemical Application of Infrared Spectroscopy; Academic Press: New York, 1963.
26. Sartori, C.; Finch, D. S.; Ralph, B.; Gilding, K. Polymer 1997, 38, 43.
27. Chavasit, V.; Kienzle-Sterzer, C.; Torres, J. A. Polym Bull 1988, 19, 223.